Friction **12**(6): 1119–1132 (2024)
https://doi.org/10.1007/s40544-023-0760-8
ISSN 2223-7690
CN 10-1237/TH
RESEARCH ARTICLE

Atomistic understanding of rough surface on the interfacial friction behavior during the chemical mechanical polishing process of diamond

Song YUAN, Xiaoguang GUO, Hao WANG, Renke KANG, Shang GAO*
State Key Laboratory of High-performance Precision Manufacturing, Dalian University of Technology, Dalian 116024, China
Received: 01 January 2023 / Revised: 11 February 2023 / Accepted: 15 March 2023

Abstract: The roughness of the contact surface exerts a vital role in rubbing. It is still a significant challenge to understand the microscopic contact of the rough surface at the atomic level. Herein, the rough surface with a special root mean square (RMS) value is constructed by multivariate Weierstrass–Mandelbrot (W–M) function and the rubbing process during that the chemical mechanical polishing (CMP) process of diamond is mimicked utilizing the reactive force field molecular dynamics (ReaxFF MD) simulation. It is found that the contact area A/A_0 is positively related with the load, and the friction force F depends on the number of interfacial bridge bonds. Increasing the surface roughness will increase the friction force and friction coefficient. The model with low roughness and high lubrication has less friction force, and the presence of polishing liquid molecules can decrease the friction force and friction coefficient. The RMS value and the degree of damage show a functional relationship with the applied load and lubrication, i.e., the RMS value decreases more under larger load and higher lubrication, and the diamond substrate occurs severer damage under larger load and lower lubrication. This work will generate fresh insight into the understanding of the microscopic contact of the rough surface at the atomic level.

Keywords: diamond; random roughness; reactive force field molecular dynamics (ReaxFF MD); friction; Weierstrass–Mandelbrot (W–M) function; chemical mechanical polishing (CMP)

1 Introduction

Chemical mechanical polishing (CMP) is a significant machining method to acquire ultra-smooth surface at the atomic level, which can realize the flattening of materials. It is also one of the key technologies for semiconductor wafer machining. However, the ultra-wide-band-gap semiconductor devices put forward extremely harsh processing requirements for the machining of single crystal diamond: sub-nanometer roughness, nanometer profile accuracy, and ultra-low damage. Tribology is defined as the science and technology of studying the theory and practice of binary surfaces with relative motion and interaction. It can be utilized to study the effects of friction, wear, and lubrication between interacting surfaces during rubbing, as well as the effects of surface chemical modifications on tribological properties [1–3]. From a micro point of view, the polishing process involves the dynamic friction process between the abrasive and the substrate. Thus, it is of great significance for elucidating the removal mechanism to understand the friction behavior at the atomic level in the polishing process. Since no two real surfaces in actual contact are perfectly fit, the abrasive and the workpiece only contact at a few microscopic points on their surfaces. The real contact area is less than the theoretical contact area, so a higher contact pressure will occur [4, 5].

* Corresponding author: Shang GAO, E-mail: gaoshang@dlut.edu.cn

The initial roughness of the contact surface is a key factor affecting the surface quality in machining. It affects the interfacial friction force F and oxidation degree by impacting the real contact area.

At the macro level, it has long been known that friction force is positively related to the load and has nothing to do with the real contact area. The friction coefficient μ (= F/F_N) is defined by the proportional relationship between the normal load F_N and the F [6]. At the macro scale, the classical law of friction (proposed by Amontons and Coulomb et al.) held that the friction force is proportional to the applied load and independent of the surface contact area, and the friction coefficient only depends on the material properties regardless of the surface contact area, sliding speed, and load [7]. According to Bowden and Tabor's friction model [6], tangential force is directly proportional to the real contact area and correlates to the shear strength of contact surface. Moreover, the friction coefficient is not just the material parameter, and it also relies on two contacting materials. However, because the continuum model cannot apply to the atomic scale, the physical mechanism behind the friction coefficient is still not fully understood. As one of the most well-known methods for assessing the atomic scale, the molecular dynamics (MD) simulation is an available path to exploring the friction process at the micro scale.

Many scholars have studied the friction mechanism at the atomic level. Several studies have shown that when the friction law extends to the atomic level, friction force is linearly correlated with the real contact area at the specific condition of rigid abrasive and rigid substrate. The MD simulation results that under different loads, the rigid solid contacted with the random rough body as well as the flat surface showed that the contact area changed linearly under the condition of small loads. For high loads, the contact area tended to fullness, and the interfacial separation tended to zero. For the super smooth surfaces, full contact could be achieved at the condition of moderate loads without solid plastic deformation [8]. Aiming at the elastic body and the rigid body, Campañá et al. [9] gave the relationship between the contact area and the normal force. Below the threshold, the contact area and friction force followed the Hertz contact theory, and the contact area and load were linearly dependent. Later, Spijker et al. [10] constructed an MD model of aluminum substrate with rough surface, which allowed the substrate to undergo free deformation and adhesion during rubbing. They demonstrated that the contact area increased proportionally with the increasement of applied load, and the roughness decreased with the increasement of contact area. The models in the previous studies included the dry contact rubbing model of three-dimensional rough surface [10, 11], the rubbing models of two ideal surfaces [12–15], the rubbing models between single rough body and ideal surface [16, 17], the rubbing process between amorphous materials [18], and thin film model of two-dimensional rough surface [19]. However, they do not take into account the role of lubricants in the contact of three-dimensional rough surface during compression and rubbing. On the surface with roughness, lubricants and polishing liquid could enter the concave body, while other convex surfaces make heavy contact under F_N [17, 20]. In the mixed lubrication state, the two friction surfaces interact through the contact between the ultra-thin lubrication layer and the rough body, resulting in elastoplastic deformation and fracture. Due to the rough surface at the atomic scale, the macroscopic friction law does not apply to the nanoscale contact [1], and it has become the focus of many scholars to further study the effects of atomic roughness on friction and adhesion. For example, Delogu [21] illustrated that when two Ni substrates with rough surface collided, local atoms would rearrange, and mechanical stress would dissipate the mechanical energy at the contact point of convex peaks. Kim and Strachan [22] proposed that the strength of the maximum contact length between two platinum surfaces with nanoscale roughness was intensely dependent on size. The contact area increased proportionally with the load, and under a constant load, enhancing surface roughness reduced the contact area. F_N would result in the variations of surface roughness [10]. Over the years, the MD models with single and multiple rough bodies have confirmed the linear relation between friction force and load [10, 11, 23, 24], and atomic roughness is applied to investigate the effects on rubbing. It is observed that smaller roughness can prevent interfacial rubbing, and thus

enhance friction force [19, 25]. One MD model of diamond rubbing with contact intervals model proposed by Zhang et al. [26] concluded that the difficulty and adhesion of atom/ion transfer and the difference in contact area led to different force response. Since the contact gap may have obvious force response and separation effect, the continuous friction behavior occurring at the fretting interface mainly lies in the friction gap and interfacial separation. In view of all that has been mentioned so far, it is still a major challenge to understand the microscopic contact mechanism of the rough surface from an atomic perspective.

To date, numerous literatures have investigated the friction mechanism of diamond CMP [27], silicon [28], copper [29], and other materials. The previous literatures established an ideal smooth surface, but there was no study on deformable surface sliding with random roughness. From a macroscopic point of view, the rough surfaces should be focused more priority, as the actual surfaces in contact are rough and deformable and occur wear and plastic deformation. At the atomic scale, mixing lubrication involves the contact of nano-rough bodies, in which the load is not only supported by rough bodies, but also limited by lubricant support. To simulate the CMP process of diamond, the first step in this process was to construct the rough surface with a special root mean square (RMS) value by using the multivariate Weierstrass–Mandelbrot (W–M) function method, and then the reactive force field molecular dynamics (ReaxFF MD) model of diamond CMP was established. Finally, the rubbing process of two rough deformable surfaces was simulated, and the friction mechanism of the rough surface from the perspective of the atomic level was explored by changing the number of lubricating molecules, the surface roughness, and the load.

2 Methodology

2.1 Model construction with random rough surface

The W–M function developed by Ausloos and Berman [30] can establish the random rough surface in three-dimensional space. The form can be represented by Eq. (1): $z(x,y)$ is the random rough surface in three-dimensional space in the height of the specified point.

$$z(x,y)=C\sum_{m=1}^{M}\sum_{n=0}^{n_{\max}}\gamma^{(Ds-3)n}\left\{\cos\Phi_{m,n}-\cos\left[\frac{2\pi\gamma^{n}\sqrt{x^2+y^2}}{L_{\max}}\cos\left(\tan^{-1}\left(\frac{y}{x}\right)-\frac{\pi m}{M}\right)+\Phi_{m,n}\right]\right\} \tag{1}$$

The idea of this function can be understood as a two-dimensional fractal section as a "ridge", and then the "ridge" of different angles and ranges is superimposed to form a random surface. M in Eq. (1) is the number of "ridge", $n_{\max}$ is the "ridge" frequency, m and n represent the values of M and $n_{\max}$ in the summation symbolic, respectively, and the parameter of γ controls the amplitude and frequency of the cosine shape and is set to 1.5. Ds is the fractal dimension set between 2 and 3 for the three-dimensional space [31]. $\Phi_{m,n}$ is a random phase array based on the random value between 0 and 2π, used to prevent the cosine function in the frequency of geometric overlap. $L_{\max}$ represents the size of the sample, G is used for scaling of the surface roughness coefficient of amplitude, and C is the scale factor, and its mathematics is shown in Eq. (2).

$$C=L_{\max}\left(\frac{G}{L_{\max}}\right)^{Ds-2}\left(\frac{\ln\gamma}{M}\right)^{\frac{1}{2}} \tag{2}$$

Firstly, the rough surface with a specified RMS value was constructed by the W–M method, and then the continuous rough surface was divided into discrete data according to a mesh size of 1 Å × 1 Å, and the RMS value of the data was calculated. Finally, the surface was mapped into the generated Large-scale Atomic/Molecular Massively Parallel Simulator (LAMMPS) model, the atoms higher than the surface were deleted, and the process from mathematical form to model mapping was completed [32]. The random rough surface is generated by adjusting C, G, and sample size in the W–M function. The roughness of the diamond surface in the rubbing process R_q is calculated by the following theoretical calculation equation (Eq. (3)):

$$R_q=\sqrt{\frac{\sum_{i=1}^{N}z_i^2}{N}} \tag{3}$$

In Eq. (3), z_i is the height of the surface particle i, and N is the total number of particles on the diamond surface. This method uses model mapping to generate the random rough surface model.

2.2 Model construction of ReaxFF MD for diamond CMP

The ReaxFF MD method was configured to mimic the diamond CMP process. The model consisted of the diamond substrate with a size of 53.5 Å × 53.5 Å × 30 Å, the diamond abrasive with a size of 53.5 Å × 53.5 Å ×25 Å, and Fenton solution as the polishing fluid. 400H_2O, 40H_2O_2, and 40Fe^{2+} molecules as well as 200H_2O, 20H_2O_2, and 20Fe^{2+} molecules were selected to simulate high and low lubrication, respectively. The proportion of molecules in the solution was chosen by experiments [33]. To determine the influence of rough surface on the rubbing process, the above W–M method was used to construct the rough surface of diamond substrate with RMS = 0.5 nm and the rough surface of the diamond abrasive with RMS = 0.5 nm. The friction processes of smooth and rough surfaces (named as the single asperity model) and rough and rough surfaces (named as the double asperity model) were simulated. The diamond CMP is depicted in Fig. 1, and the details can be discovered in Refs. [27, 34]. Primarily, the initial equilibrium was performed under NVT ensemble with the temperature of 300 K. To avoid the high momentum produced via the rapid decline of the abrasive due to the direct application of load, a downward constant speed of 20 m/s was configured to the rigid movable layer of the diamond abrasive. When the force in the rigid movable layer reached the set value, the downward pressure was stopped. At the same time, the targeted force was imposed to the rigid movable layer. Afterwards, the diamond abrasive contacted with the diamond substrate and slid along the positive direction of the x axis to mimic the rubbing processing. The loads applied in the polishing model were 1,360, 2,040, 2,720, and 3,400 nN. The diamond abrasive slid for 200 ps with a sliding speed of 50 m/s. To rule out the boundary effect and simulate the rubbing of the abrasive in the diamond substrate for multiple times, the periodic boundary conditions were configured in the x and y directions, and the fixed boundary conditions were set in the z direction. A reflecting wall was set in the z direction to avoid the loss of atoms or interaction with the carbon atoms below [35]. The simulations were performed in NVT ensemble with a timestep of 0.25 ps, the temperature of the control system was 300 K with a coefficient of 25 fs by the Nose–Hoover thermostat [36, 37], and the motion equation of particles was calculated utilizing the velocity verlet algorithm [38]. The C/H/O/Fe potential function in ReaxFF [39] has been provided to investigate the rubbing mechanism of the diamond CMP process [27, 34, 40]. The MD calculations were performed in LAMMPS [41, 42], and Open Visualization Tool (OVITO) [43] was used for visualization and analysis in the later stage. Due to the limitations of current computing power, a higher sliding speed was widely used [44–48]. The friction values in Section 3 were output per 0.1 ps, sampled at 0.025 ps of intervals, and averaged from 40 data points.

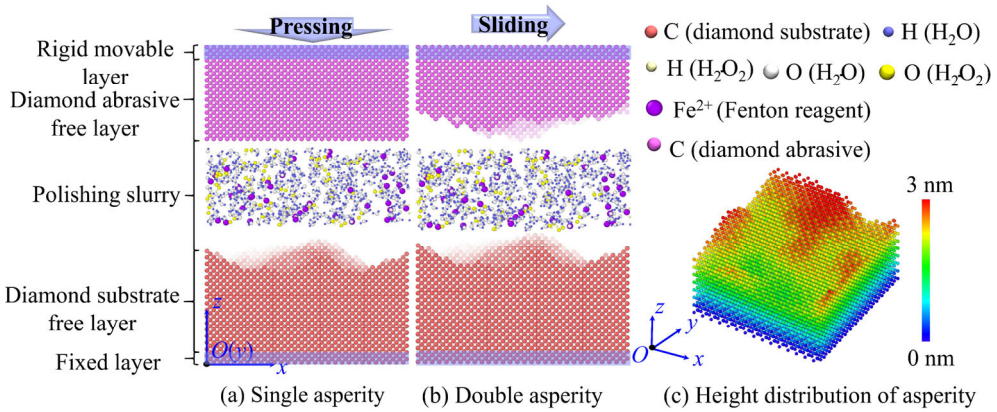

Fig. 1 ReaxFF MD model of diamond CMP with random rough surface.

3 Results and discussion

3.1 Contact between rough surface under different loads

In the single asperity contact, it is found that the contact area relies on the load in the MD simulations [49]. Herein, the formation of bridge bonds between the diamond abrasive and the diamond substrate is regarded as the basis for judging the contact. The number of the carbon atoms in one layer of x–y plane is regarded as the A_0, the number of the carbon atoms forming bridge bonds is regarded as the avail A, and the contact area is defined by A/A_0. Figure 2 shows the numbers of bridge bonds under single and double asperity models after pressure equilibrium for 25 ps. According to the number of bridge bonds formed, the plots of A/A_0 under different loads in the single and double asperity model are drawn, as shown in Fig. 3. There is little discrepancy regarding the contact area between the two models under low loads. However, what is interesting about the data in Fig. 3 is that under high loads, the contact area in the double asperity model gradually increases, while the contact area in the single asperity model gradually stabilizes with the increasement of load, as shown in Fig. 3(a). It can be explained by the fact that the rough surface begins to be compressed after the larger load imposes on the system. In the double asperity model, the polishing liquid molecules enter the cavity of the surface and cannot form a lubricating layer between the abrasive and the substrate. Nonetheless, more polishing liquid molecules are adsorbed on the smooth surface of the abrasive in the single asperity model, and a lubricating layer occurs between the abrasive and the substrate, which prevents the increasement of the contact area between the abrasive and the substrate. When the number of polishing liquid molecules is very small, part of the polishing liquid is adsorbed on the smooth surface of the abrasive, resulting in the contact area in the single asperity model less than that in the double asperity model. Most of the polishing liquid molecules enter into the cavity, and the single and double asperity models only rely on the convex peak of the rough surface to bear the pressure. Therefore, the contact

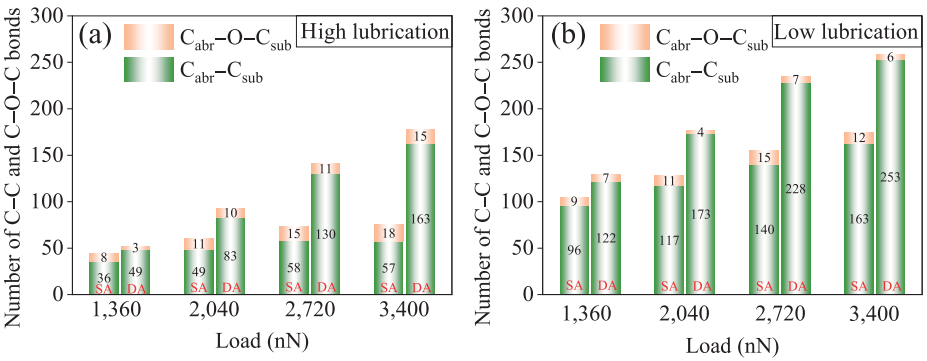

Fig. 2 Numbers of interfacial bridge bonds under different loads. Note: SA and DA here mean single asperity and double asperity, respectively, and the carbon atoms from the substrate and abrasive are abbreviated as C_{sub} and C_{abr}, respectively.

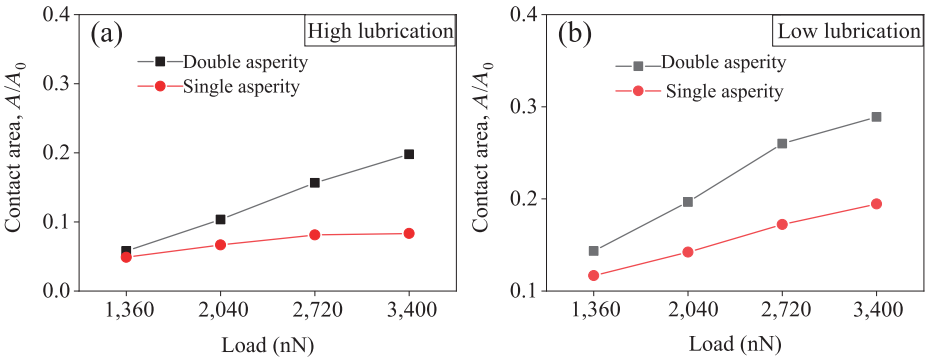

Fig. 3 A/A_0 between abrasive and substrate under different loads.

area in both the single and double asperity models increases with the increasement of the load, as depicted in Fig. 3(b).

3.2 Effects of surface roughness on interfacial friction behavior

It can be concluded from the friction curves (Figs. 4(a) and 4(b)) that under the same load, the single asperity model has less friction force, which indicates that the friction force is not directly correlated to the load, but to the surface roughness. Figures 5(c) and 5(d) represent the variation curves of the number of C–C and C–O–C bridge bonds with the sliding time. Due to the discrepancy of bond strengths between C–O and C–C being 1,077 and 610 kJ/mol, respectively, [50, 51], more energy is needed to form the C–O–C bridge bonds than the C–C bridge bonds between the abrasive and the substrate. On account of the high energy required, the system cannot supply enough energy continuously, so the number of the C–O–C bonds is in the dynamic change of formation and breakage and presents a large fluctuation.

In the single asperity model, one interesting finding is that the number of interfacial bridge bonds is lower than that in the double asperity model, that is, the contact area of the single asperity model is lower than that of the double asperity model. The friction force in the single asperity model is smaller under the same load, indicating that the friction force at the microscopic scale has nothing to do with the vertical load and is positively correlated with the real contact area. This is also consistent with the equation of $F_f = \tau A_{real} N_{atom}$ (where τ is the interfacial shear strength, A_{real} is the surface area per atom, and N_{atom} is the number of atoms in contact) proposed by Mo et al. [23]. In the single and double asperity models, the same phenomenon is that the friction force is positively correlated with the applied load, and the number of interfacial bridge bonds also increases with the increasement of the applied load. This also manifests that the number of atoms in real contact increases under a larger load, thus increasing the interfacical friction force. More interestingly, the friction coefficient increases primarily, and then decreases during the rubbing process, as shown in Figs. 4(c) and 4(d). In the single asperity model, the friction coefficient increases slowly, and then decreases slowly regardless of the loads. Nevertheless, in the double asperity model, while rubbing under a low load, the friction coefficient increases quickly with a large enhancement, and then decreases rapidly; while rubbing under high loads, the friction coefficient increases slowly, and then

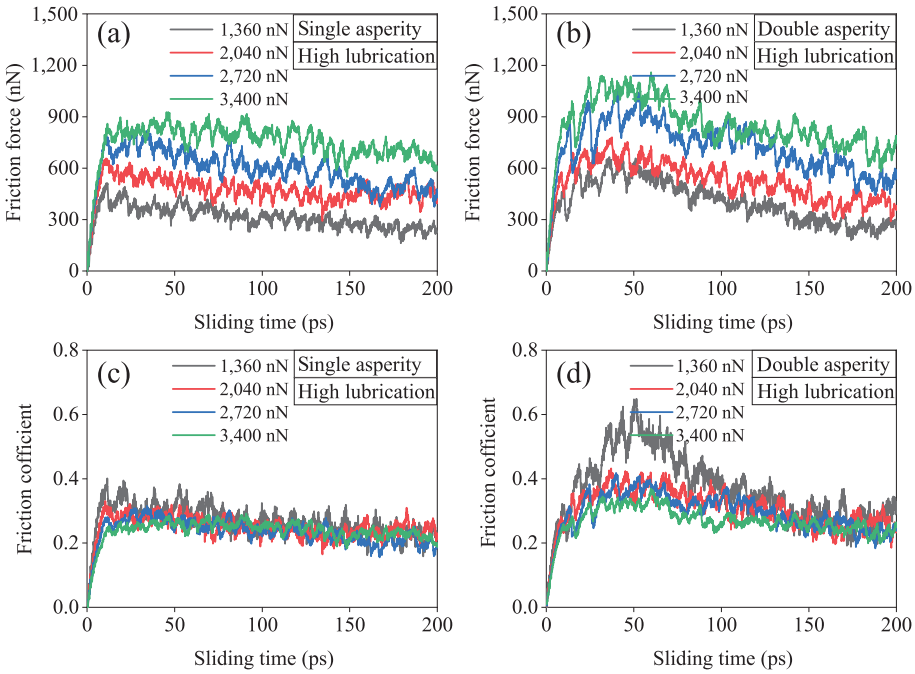

Fig. 4 Variation curves of friction force and friction coefficient during sliding.

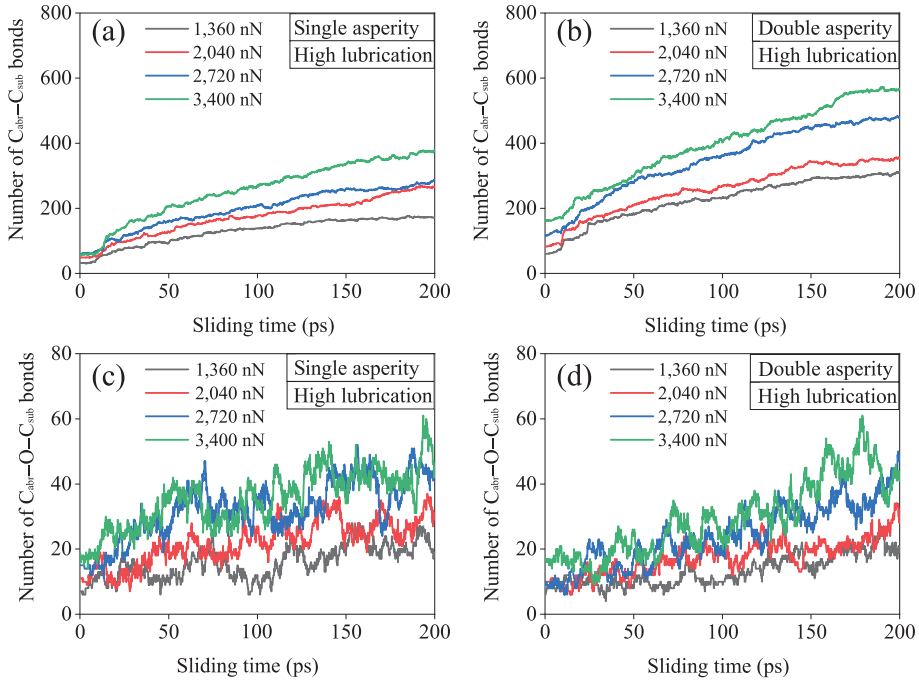

Fig. 5 Plots of number of C–C and C–O–C bonds over sliding time.

decreases gradually. In the double asperity model, the contact of convex peak between the abrasive and the substrate under a low load results in a small contact area. At the beginning of sliding, the contact area of convex peak first increases, which leads to a rapid increase in the friction coefficient. The convex peak begins to be removed with the sliding time, causing a gradual reduction in the real contact area between the abrasive and the substrate. While the convex peak is completely removed, the free amorphous carbon atoms fill up the cavity, and finally the friction coefficient decreases until it is stabilized. Nonetheless, under high loads, the convex peak between the abrasive and the substrate is squeezed by a large load, which makes the abrasive and the substrate have fuller contact at the initial stage of sliding. Thus, the increasement of friction coefficient in the rubbing process is small. In the later stage of rubbing, after sufficient rubbing, a free amorphous carbon layer is formed between the abrasive and the substrate. Nevertheless, in the single asperity model, the friction coefficient of the whole system will not fluctuate greatly regardless load, indicating that it is in a relatively stable friction system at this time, and it is easier to realize ultra-smooth sliding on the low rough surface. The friction coefficient is not a constant coefficient at the microscopic scale and is related to the roughness of the contact surface. It is also found that when the load is applied, the polishing liquid molecules can fill up the cavity and sustain the load, thus reducing the contact area and protecting the surface morphology.

3.3 Effects of polishing fluid lubrication on interfacial friction behavior

To compare the discrepancy between the high lubrication and low lubrication, we only change the number of polishing fluid molecules based on the above model, and the relevant friction force and friction coefficient were calculated, as presented in Fig. 6. It is observed from the data in Fig. 6 that under low lubrication, the friction force in the double asperity model is larger than that in the single asperity model. The friction force under low lubrication is also larger than that in the high lubrication model.

Similarly, we have calculated the number of bridge bonds with time during the sliding process under different loads, as seen in Fig. 7. There is a clear trend that the number of bridge bonds is positively correlated with the friction force, proving that the equation of $F_f = \tau A_{real} N_{atom}$ is also applicable under low lubrication. Under high lubrication, the friction decreases slightly

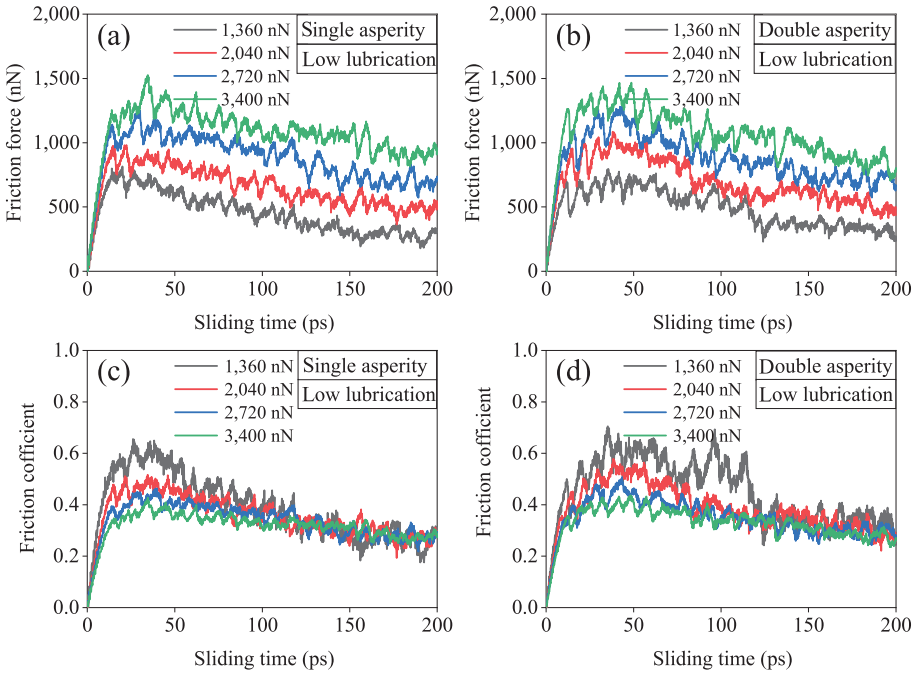

Fig. 6 Variation curves of friction force and friction coefficient during rubbing under low lubrication.

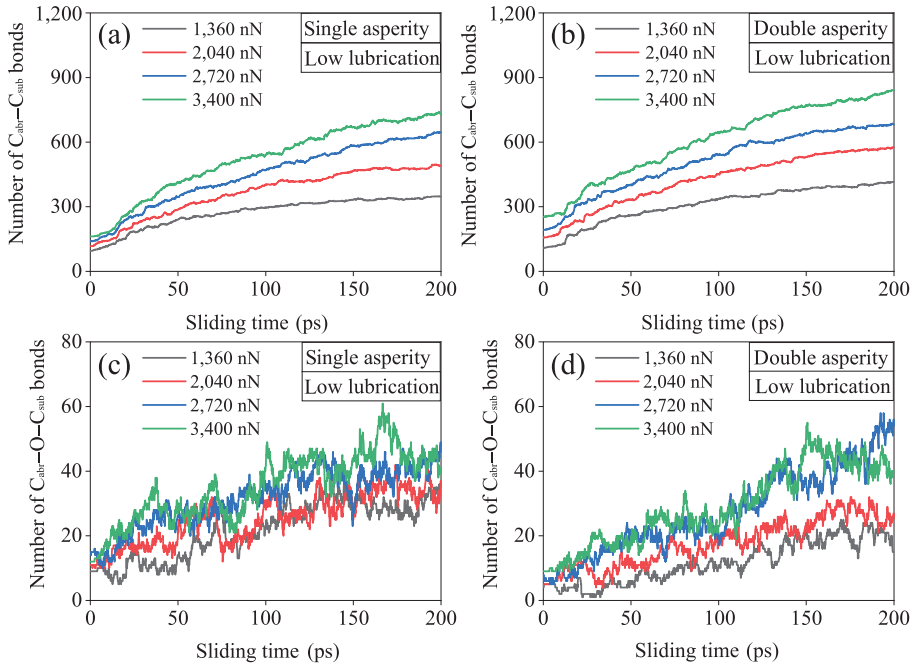

Fig. 7 Curves of number of C–C and C–O–C bridge bonds with sliding time under low lubrication.

at the later stage of rubbing, as seen in Fig. 4; while under low lubrication, the friction force decreases dramatically at the later period of rubbing, and this phenomenon is more obvious in the double asperity model. A possible explanation for this might be that the huge friction force leads to intense mechanochemical interactions between the abrasive and the substrate. In comparison with diamond, diamond-like carbon film has a lower friction coefficient, and a higher pressure can make more diamond atoms convert to amorphous carbon atoms. Therefore, the friction force at the interface tends to decrease more significantly at a higher pressure [27, 52–55]. Under low lubrication, the lubricant molecules cannot completely fill up

the cavity and sustain the load, and the surface morphology cannot be effectively protected. A thicker amorphous carbon lubrication layer is formed between the abrasive and the substrate. Compared with the original structure, the initial convex peak is not only gradually flattened, but also the intact lattice of the subsurface is damaged after 200 ps of rubbing. In the model with high lubrication and single asperity, the substrate has minimal damage. In the model with low lubrication and double asperity, the convex peaks of the substrate are almost all removed, and severe damage layers also appear, as seen in Fig. 8.

Figure 9 shows the comparison of friction coefficients under different models and loads. According to the averaged friction coefficients, it is apparent that the double asperity model has a large friction coefficient under a small load, and the friction coefficient reduces rapidly with the increasement of load. This result can be explained by the fact that the convex peak of the rough surface is compressed in the compression process, so that the contact area in the rubbing process changes. Additionally, the polishing liquid molecules adsorb on the surface of the diamond abrasive and the diamond substrate, which weakens the influence of rough contact on friction force, thus reducing the friction coefficient. When the load is greater than 2,040 nN, the friction coefficient is in line with the load in several models, and it decreases with the increasement of the load. Under the double asperity model, it exists the highest friction coefficient, and the presence of lubricant molecules can also reduce the friction coefficient, which indicates that the friction coefficient can be effectively reduced by the surface with high lubrication and low roughness.

3.4 Changes of subsurface damage thickness and RMS value after rubbing

In Fig. 10, we can see that the number of amorphous carbon atoms decreases first, and then increases at the beginning of the sliding process. In the period of pressure equilibrium, due to the direct contact extrusion between convex peaks, the run-in period occurs. At 0 ps, the convex peaks between the abrasive and the substrate contact each other. In this case, there is no friction force along the rubbing direction, and only an extrusion pressure exists in the z direction. Elastic deformation occurs when the convex peaks in contact are squeezed. After the rubbing starts, the contact convex peaks begin to separate, the contact area gradually changes from the cusp contact of convex peak to the side contact of convex peak, and the elastic recovery of some atoms squeezed at the cusp leads to the temporary decline of the number of amorphous atoms. This phenomenon is particularly obvious under the condition of high load and low lubrication in the single asperity model. In the single asperity model, the abrasive has more contact with the convex peak in the substrate. As the rubbing progresses,

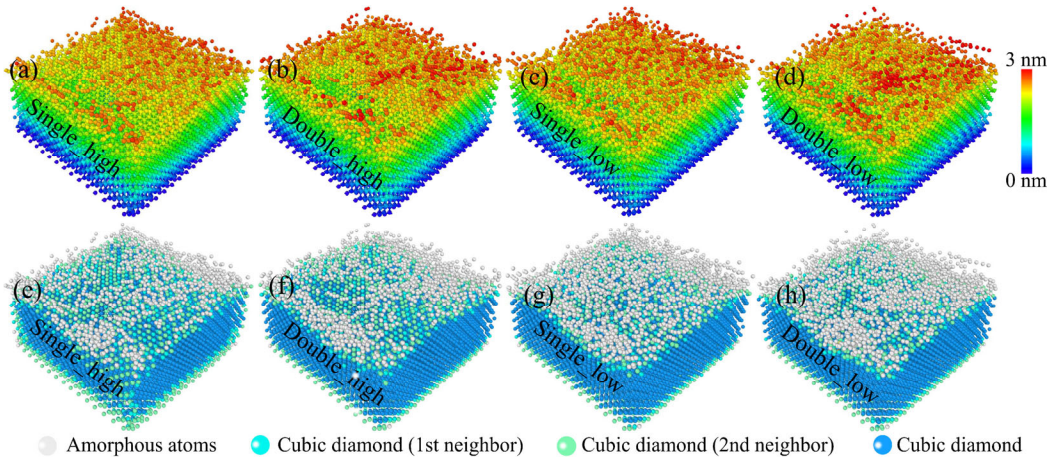

Fig. 8 Snapshots of diamond substrate after 200 ps of rubbing at the load of 2,720 nN: (a) height distribution of single asperity and high lubrication, (b) height distribution of double asperity and high lubrication, (c) height distribution of single asperity and low lubrication, (d) height distribution of double asperity and low lubrication, (e) snapshots of amorphous atoms in single asperity and high lubrication, (f) snapshots of amorphous atoms in double asperity and high lubrication, (g) snapshots of amorphous atoms in single asperity and low lubrication, and (h) snapshots of amorphous atoms in double asperity and low lubrication.

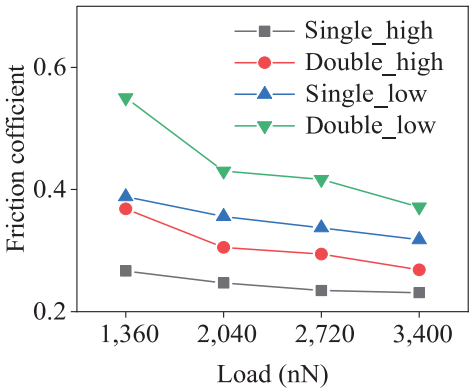

Fig. 9 Comparison of averaged friction coefficients under different models and loads (the data are sampled from the average of 100 ps after rubbing).

the substrate begins to appear damage, and a large number of amorphous carbon atoms gradually appear.

The results of the correlational analysis show that the single asperity model has small friction force and friction coefficient under high lubrication. We compare the damage degree and RMS value of diamond substrate under several simulated conditions. The variations of RMS roughness of diamond substrate after rubbing for 200 ps are provided in Fig. 11. Due to rubbing effects and loads, the RMS roughness of each system shows a decreasing trend. The variations of RMS and the damage degree of diamond substrate after rubbing show a relationship with the applied load, i.e., the reduction degree of RMS and the damage degree of diamond substrate increase with the successive increasement of load. Under low lubrication, the RMS decreases intensely, but the diamond substrate also has a large degree of damage simultaneously. Under the low lubrication condition, there is nearly no difference in the RMS in the single and double asperity models, especially in the case of large load. However, larger damage will appear in the double asperity model. Under the high lubrication, the relatively smooth between the abrasive and the substrate can realize efficient ultra-smooth removal more easily.

4 Conclusions

The ReaxFF MD models of diamond CMP with single asperity and double asperity were constructed, and the friction mechanisms of the diamond CMP process under different loads and lubrication conditions were studied.

In CMP, the diamond abrasive contacts with the diamond substrate, making the carbon atoms in the diamond substrate deform. In favor of the abrasive, the energy of carbon atoms in the diamond substrate increases, indirectly reducing the activation energy of

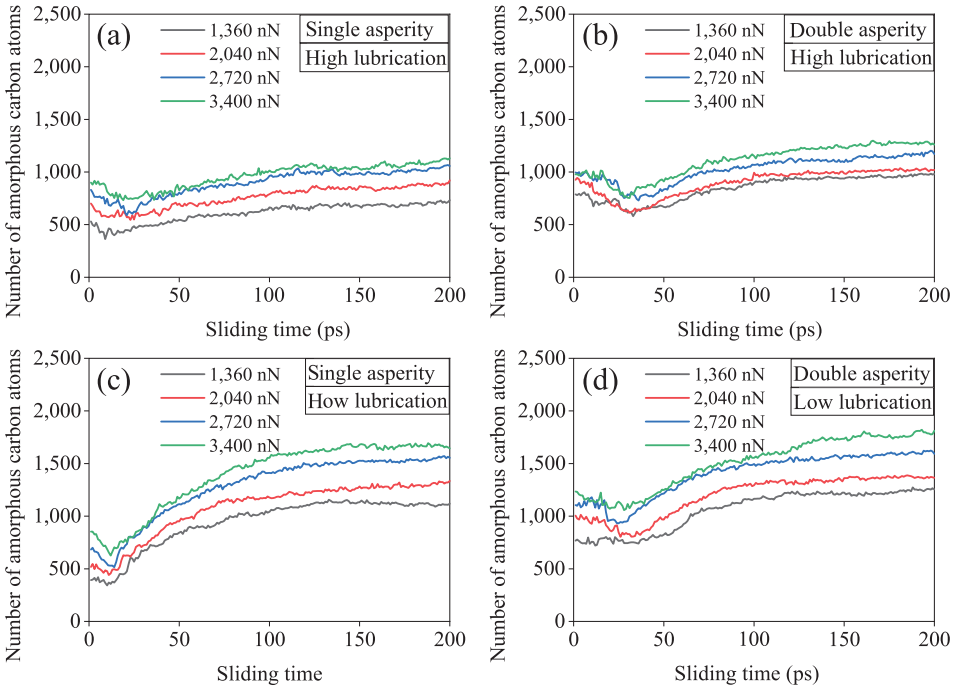

Fig. 10 Variation curves of amorphous atoms over sliding time under different conditions.

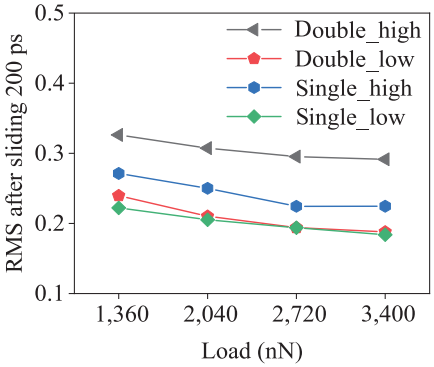

Fig. 11 Variations of RMS roughness of diamond substrate after rubbing for 200 ps.

the chemical reaction, so as to form the carbon atoms with high activity. The stronger the mechanical force caused by the abrasive and polishing pressure, the higher the energy of the activated carbon atoms, and the easier to react with the polishing fluid. The formation process of the C–C bridge bonds is as follows: Firstly, the •OH reacts with the diamond substrate to form the C–OH structure, and then the •OH will fall off from the diamond substrate, making the carbon atoms contacting with the •OH more active. Finally, the activated carbon atoms will easily form the C–C bridge bonds with the carbon atoms in the diamond abrasive. The formation process of the C–O–C bridge bonds is as follows: Firstly, the •OH reacts with the diamond substrate to form the C–OH structure, and then the H in the •OH will fall off under mechanical force of the diamond abrasive, making the oxygen atoms more active. Finally, the activated oxygen atoms will easily form the C–O–C bridge bonds with the carbon atoms in the diamond abrasive.

This study also shows that the contact area between the diamond abrasive and the diamond substrate increases in proportion to the F_N, and the friction force depends on the number of interfacial bridge bonds, indicating that the relationship between the friction force and the contact area can be expanded to the atomic scale. The occurrence of numerous lubricating molecules can decrease the interfacial friction force and friction coefficient. The friction force is not directly related to the load, but is related to the surface roughness. Lubricant molecules can fill up the cavity, and then sustain the load and cause a smaller contact area, so as to protect the surface topography. Under the same load, increasing the surface roughness will decrease the contact area between the diamond abrasive and the diamond substrate, which also manifests that it is easier to realize ultra-smooth rubbing on the surface with low roughness. The findings may shed new light on the understanding of the microscopic contact of the rough surface and be of assistance to achieve atomic-level machining of diamond.

Acknowledgements

The authors greatly appreciate the financial support of the National Key R&D Program of China (2022YFB3404304) and the National Natural Science Foundation of China (No. 5217052183). The authors acknowledge Beijng PARATERA Tech Corp., Ltd., China, for providing high-performance computing (HPC) resources that have contributed to the research results reported within this paper.

Declaration of competing interest

The authors have no competing interests to declare that are relevant to the content of this article.

References

[1] Zhang Z N, Yin N, Chen S, Liu C L. Tribo-informatics: Concept, architecture, and case study. *Friction* **9**(3): 642–655 (2021)

[2] Yin N, Xing Z G, He K, Zhang Z N. Tribo-informatics approaches in tribology research: A review. *Friction* **11**(1): 1–22 (2023)

[3] Pan S H, Jin K Y, Wang T L, Zhang Z N, Zheng L, Umehara N. Metal matrix nanocomposites in tribology: Manufacturing, performance, and mechanisms. *Friction* **10**(10): 1596–1634 (2022)

[4] Huang P. *Tribology Course*. Beijing: Higher Education Press, 2008. (in Chinese)

[5] Lv X K, Yang W J, Xu G L, Huang X M. The influence of characteristic of rough surface on gas sealing performance in seal structure. *J Mech Eng* **51**(23): 110–115 (2015) (in Chinese)

[6] Bowden F P, Tabor D. *The Friction and Lubrication of Solids*. Oxford, UK: Oxford University Press, 2001.

[7] Gao S, Li H G, Huang H, Kang R K. Grinding and lapping induced surface integrity of silicon wafers and its effect on chemical mechanical polishing. *Appl Surf Sci* **599**: 153982 (2022)

[8] Yang C, Persson B N J. Molecular dynamics study of contact mechanics: Contact area and interfacial separation from small to full contact. *Phys Rev Lett* **100**(2): 024303 (2008)

[9] Campañá C, Müser M H, Robbins M O. Elastic contact between self-affine surfaces: Comparison of numerical stress and contact correlation functions with analytic predictions. *J Phys-Condens Mat* **20**(35): 354013 (2008)

[10] Spijker P, Anciaux G, Molinari J F. The effect of loading on surface roughness at the atomistic level. *Comput Mech* **50**(3): 273–283 (2012)

[11] Spijker P, Anciaux G, Molinari J F. Dry sliding contact between rough surfaces at the atomistic scale. *Tribol Lett* **44**(2): 279–285 (2011)

[12] Gao J P, Luedtke W D, Landman U. Layering transitions and dynamics of confined liquid films. *Phys Rev Lett* **79**(4): 705–708 (1997)

[13] Sivebaek I M, Samoilov V N, Persson B N J. Velocity dependence of friction of confined hydrocarbons. *Langmuir* **26**(11): 8721–8728 (2010)

[14] Berro H, Fillot N, Vergne P. Molecular dynamics simulation of surface energy and ZDDP effects on friction in nano-scale lubricated contacts. *Tribol Int* **43**(10): 1811–1822 (2010)

[15] Jabbarzadeh A, Harrowell P, Tanner R I. Very low friction state of a dodecane film confined between mica surfaces. *Phys Rev Lett* **94**(12): 126103 (2005)

[16] Gao J P, Luedtke W D, Lman U. Nano-elastohydrodynamics: Structure, dynamics, and flow in nonuniform lubricated junctions. *Science* **270**(5236): 605–608 (1995)

[17] Zheng X, Zhu H T, Kiet Tieu A, Kosasih B. A molecular dynamics simulation of 3D rough lubricated contact. *Tribol Int* **67**: 217–221 (2013)

[18] Jabbarzadeh A, Harrowell P, Tanner R I. Low friction lubrication between amorphous walls: Unraveling the contributions of surface roughness and in-plane disorder. *J Chem Phys* **125**(3): 034703 (2006)

[19] Jabbarzadeh A, Atkinson J D, Tanner R I. Effect of the wall roughness on slip and rheological properties of hexadecane in molecular dynamics simulation of Couette shear flow between two sinusoidal walls. *Phys Rev E* **61**(1): 690–699 (2000)

[20] Zheng X, Zhu H T, Tieu A K, Kosasih B. Roughness and lubricant effect on 3D atomic asperity contact. *Tribol Lett* **53**(1): 215–223 (2014)

[21] Delogu F. Molecular dynamics of collisions between rough surfaces. *Phys Rev B* **82**(20): 205415 (2010)

[22] Kim H, Strachan A. Nanoscale metal-metal contact physics from molecular dynamics: The strongest contact size. *Phys Rev Lett* **104**(21): 215504 (2010)

[23] Mo Y F, Turner K T, Szlufarska I. Friction laws at the nanoscale. *Nature* **457**(7233): 1116–1119 (2009)

[24] Szlufarska I, Chandross M, Carpick R W. Recent advances in single-asperity nanotribology. *J Phys D Appl Phys* **41**(12): 123001 (2008)

[25] Eder S, Vernes A, Vorlaufer G, Betz G. Molecular dynamics simulations of mixed lubrication with smooth particle post-processing. *J Phys Condens Matter* **23**(17): 175004 (2011)

[26] Zhang Z N, Pan S H, Yin N, Shen B, Song J. Multiscale analysis of friction behavior at fretting interfaces. *Friction* **9**(1): 119–131 (2021)

[27] Yuan S, Guo X G, Mao Q, Guo J, van Duin A C T, Jin Z J, Kang R K, Guo D M. Effects of pressure and velocity on the interface friction behavior of diamond utilizing ReaxFF simulations. *Int J Mech Sci* **191**: 106096 (2021)

[28] Yuan S, Guo X G, Li P H, Zhang S H, Li M, Jin Z J, Kang R K, Guo D M, Liu F M, Zhang L M. Atomistic understanding of interfacial processing mechanism of silicon in water environment: A ReaxFF molecular dynamics simulation. *Front Mech Eng* **16**(3): 570–579 (2021)

[29] Shi J Q, Fang L, Sun K, Peng W X, Ghen J, Zhang M. Surface removal of a copper thin film in an ultrathin water environment by a molecular dynamics study. *Friction* **8**(2): 323–334 (2020)

[30] Ausloos M, Berman D H. A multivariate Weierstrass–Mandelbrot function. *P Roy Soc A-Math Phy* **400**(1819): 331–350 (1985)

[31] Papanikolaou M, Salonitis K. Fractal roughness effects on nanoscale grinding. *Appl Surf Sci* **467–468**: 309–319 (2019)

[32] Feng R C, Yang S Z, Shao Z H, Yao Y J, Zhang J, Cao H, Li H Y. Atomistic simulation of effects of random roughness

on nano-cutting process of γ-TiAl alloy. *Rare Metal Mat Eng* **51**(5): 1650–1659 (2022)

[33] Yuan S, Guo X G, Lu M G, Jin Z J, Kang R K, Guo D M. Diamond nanoscale surface processing and tribochemical wear mechanism. *Diam Relat Mater* **94**: 8–13 (2019)

[34] Yuan S, Guo X G, Huang J X, Gou Y, Jin Z J, Kang R K, Guo D M. Insight into the mechanism of low friction and wear during the chemical mechanical polishing process of diamond: A reactive molecular dynamics simulation. *Tribol Int* **148**: 106308 (2020)

[35] Assowe O, Politano O, Vignal V, Arnoux P, Diawara B, Verners O, van Duin A C T. Reactive molecular dynamics of the initial oxidation stages of Ni(111) in pure water: Effect of an applied electric field. *J Phys Chem A* **116**(48): 11796–11805 (2012)

[36] Hoover W G. Canonical dynamics: Equilibrium phase-space distributions. *Phys Rev A* **31**(3): 1695–1697 (1985)

[37] Carter S, Handy N C. A variational method for the calculation of ro-vibronic levels of any orbitally degenerate (Renner–Teller) triatomic molecule. *Mol Phys* **52**(6): 1367–1391 (1984)

[38] Van Gunsteren W F, Berendsen H J C. Algorithms for macromolecular dynamics and constraint dynamics. *Mol Phys* **34**(5): 1311–1327 (1977)

[39] Zou C Y, van Duin A. Investigation of complex iron surface catalytic chemistry using the ReaxFF reactive force field method. *JOM* **64**(12): 1426–1437 (2012)

[40] Yuan S, Guo X G, Huang J X, Lu M G, Jin Z J, Kang R K, Guo D M. Sub-nanoscale polishing of single crystal diamond(100) and the chemical behavior of nanoparticles during the polishing process. *Diam Relat Mater* **100**: 107528 (2019)

[41] Aktulga H M, Fogarty J C, Pandit S A, Grama A Y. Parallel reactive molecular dynamics: Numerical methods and algorithmic techniques. *Parallel Comput* **38**(4–5): 245–259 (2012)

[42] Plimpton S. Fast parallel algorithms for short-range molecular dynamics. *J Comput Phys* **117**(1): 1–19 (1995)

[43] Stukowski A. Visualization and analysis of atomistic simulation data with OVITO—The Open Visualization Tool. *Modelling Simul Mater Sci Eng* **18**(1): 015012 (2010)

[44] Chen L, Wen J L, Zhang P, Yu B J, Chen C, Ma T B, Lu X C, Kim S H, Qian L M. Nanomanufacturing of silicon surface with a single atomic layer precision via mechanochemical reactions. *Nat Commun* **9**: 1542 (2018)

[45] Li X W, Wang A Y, Lee K R. Insights on low-friction mechanism of amorphous carbon films from reactive molecular dynamics study. *Tribol Int* **131**: 567–578 (2019)

[46] Li X W, Wang A Y, Lee K R. Mechanism of contact pressure-induced friction at the amorphous carbon/alpha olefin interface. *NPJ Comput Mater* **4**(1): 53 (2018)

[47] Wen J L, Ma T B, Zhang W W, van Duin A C T, Lu X C. Atomistic mechanisms of Si chemical mechanical polishing in aqueous H_2O_2: ReaxFF reactive molecular dynamics simulations. *Comput Mater Sci* **131**: 230–238 (2017)

[48] Wang Y, Xu J X, Ootani Y, Bai S D, Higuchi Y, Ozawa N, Adachi K, Martin J M, Kubo M. Tight-binding quantum chemical molecular dynamics study on the friction and wear processes of diamond-like carbon coatings: Effect of tensile stress. *ACS Appl Mater Interfaces* **9**(39): 34396–34404 (2017)

[49] Luan B Q, Robbins M O. The breakdown of continuum models for mechanical contacts. *Nature* **435**(7044): 929–932 (2005)

[50] Thomas E L H, Nelson G W, Mandal S, Foord J S, Williams O A. Chemical mechanical polishing of thin film diamond. *Carbon* **68**: 473–479 (2014)

[51] Lide DR. *CRC Handbook of Chemistry and Physics*, 82nd edn. Taylor & Francis, 2001.

[52] Dai M J. Mechanism and tribological behavior of doped diamond-like carbon films. Ph.D. Thesis. Guangzhou (China): South China University of Technology, 2016. (in Chinese)

[53] Ling X. Tribological properties and application of the diamond-like carbon films. Ph.D. Thesis. Lanzhou (China): Lanzhou University of Technology, 2013. (in Chinese)

[54] Zhang D C. Study on the tribological properties and applications of diamond and diamond-like carbon films. Master's Thesis. Shanghai (China): Shanghai Jiao Tong University, 2010. (in Chinese)

[55] Yong Q S, Wang H D, Xu B S, Ma G Z. Research status of the tribological property of diamond-like carbon films. *J Mech Eng* **52**(11): 95–107 (2016) (in Chinese)

Song YUAN. He is a Ph.D. student from School of Mechanical Engineering, Dalian University of Technology, China, focusing on the tribology theory and technology in ultra-precision machining, such as the chemical mechanical polishing and ReaxFF molecular dynamics simulations. He has published more than 30 papers, which have been cited for more than 300 times.

Xiaoguang GUO. She received her Ph.D. degree in 2008 from Dalian University of Technology, China. She is now working as a professor at School of Mechanical Engineering, Dalian University of Technology. She is the member of Extreme Manufacturing Branch of Chinese Mechanical Engineering Society, focusing on ultraprecision machining and theory regarding the hard and brittle. She has published more than 100 papers, which have been cited for more than 700 times.

Hao WANG. He is a Ph.D. student from School of Mechanical Engineering, Dalian University of Technology, China, focusing on ultra-precision machining theory and technology regarding the ultrasonic vibration assisted machining and molecular dynamics simulation. He has published more than 10 papers, many of which have been cited multiple times.

Renke KANG. He received his Ph.D. degree in 1999 from Northwestern Polytechnical University, China. He is now working as a professor at School of Mechanical Engineering, Dalian University of Technology, China. He is the member of International Committee of Abrasive Technology, focusing on ultraprecision machining and theory regarding the hard and brittle. He has published more than 380 papers, which have been cited for more than 3,800 times.

Shang GAO. He received his Ph.D. degree in 2014 from Dalian University of Technology, China. He is now working as an associate professor at School of Mechanical Engineering, Dalian University of Technology. He is the member of Extreme Manufacturing Branch of Chinese Mechanical Engineering Society, focusing on precision and ultra-precision machining technology, semiconductor manufacturing technology and equipment. He has published more than 50 papers, which have been cited for more than 400 times.